TECHNICAL ARTICLE

Design and Development of Shielded Metal Arc Welding (SMAW) Electrode Coatings Using a CaO-CaF_2-SiO_2 and CaO-SiO_2-Al_2O_3 Flux System

SUMIT MAHAJAN [1,2] and RAHUL CHHIBBER [1]

1.—Mechanical Engineering, IIT Jodhpur, Jodhpur 342037, India. 2.—e-mail: mahajan.1@iitj.ac.in

This study aims to investigate the physicochemical and thermophysical behavior of the electrode coatings produced using CaO-CaF_2-SiO_2 and CaO-SiO_2-Al_2O_3 ternary phase systems. Electrode coating compositions for welding power plant materials are either patented or not available in the public domain so researchers need to explore the flux coatings to improve the properties of welds produced. An extreme vertices design methodology was used to obtain the different flux combinations to study the effect of electrode coating constituents on weight loss, density, specific heat, change in enthalpy, thermal diffusivity and thermal conductivity. These properties play an important role in achieving better weld quality. X-ray diffraction and Fourier-transform infrared spectroscopy techniques were used to analyze the different phases present and their structural behavior. Multi-response optimization was carried out to obtain the optimum flux composition and study the effect of individual constituents and their interaction effects on the thermophysical and physicochemical properties.

INTRODUCTION

In shielded metal arc welding (SMAW) consumable electrodes, the primary function of electrode coating is to protect the molten metal from the outside environment, provide arc stability, refine the weld pool, etc. Electrode coatings can be made up of different types of fluxes (acidic, basic and neutral), which affect the slag properties such as density, viscosity, electrical conductivity, thermal expansion and melting temperature. The formulation of weld coatings has a major influence on the mechanical properties of the final weld.[1,2] The dissimilar metal joints are operated at a high temperature in the power plant industries and are very prone to failure. One of the factors involved is the selection of welding methods and welding consumables. Therefore, the effect of coatings on the behavior on the weld properties is of great concern. To understand the effects of welding consumables on the weld deposit properties, the prediction of the thermophysical and physicochemical properties of fluxes has interested researchers in the past few years. The heat-affected zone (HAZ) is one of the critical parts of the weld joints in austenitic/ferritic steels where the majority of failures occur. The mechanical performance of the weld is greatly affected by the chemical composition and type of electrode coating. Various physicochemical properties such as grain size, density, viscosity, thermal conductivity, surface tension, thermal diffusivity, enthalpy, specific heat and weight loss influence the quality of weld joints.[3–5] The extreme vertices design procedure is generally used by various researchers to conduct experiments with mixtures when several factors and constraints are considered.[6–11] Electrode coating ingredients help to release gases that provide the shielding to the weld pool to avoid contamination and stabilize the arc. Calcite addition is beneficial to control the weld metal hydrogen content but has a harmful effect on bead appearance. It helps to reduce the diffusible hydrogen content in welds and increases the basicity, which leads to better mechanical properties and cleaner welds. Fluorspar, a source of CaF_2, reduces the density of the flux mixture and also helps to decrease the melting point but adversely affects the slag detachability. The oxygen content in welds is

also an important concern for the weld performance, and the higher basicity of fluxes results in a lower oxygen content. It is a difficult task to understand how coatings work and how their constituents contribute to various aspects of its behavior.[12–25] Sharma et al.[26,27] estimate the physicochemical and thermophysical properties of different welding fluxes and slags containing different minerals. It was found that the CaO·TiO2 binary mixture affects the density, improves slag detachability and reduces the hydrogen content in the weld to improve weld performance. $SiO_2 \cdot Al_2O_3$ binary improves the thermal conductivity because of the network-forming nature of silica and alumina.

The aim of this study is to develop different electrode coating mixtures with higher basicity using different minerals. To design 21 sets of the electrode coating formulation, the extreme vertices methodology was used. Experiments were conducted to find the density, ΔH (change in enthalpy), $\Delta W\%$ (weight loss), thermal conductivity, specific heat and thermal diffusivity using DSC-TGA and a hot disk apparatus. Phase formation and structural behavior were investigated using x-ray diffraction (XRD) and Fourier-transform infrared spectroscopy (FTIR) techniques. Adequacy was checked using analysis of variance after developing regression models for various thermophysical and physicochemical properties in terms of flux ingredients. Effects of flux ingredients on different properties have been analyzed and discussed, and multi-objective optimized solutions have been proposed for the different flux formulations.

EXPERIMENTATION

Minerals used to prepare different electrode coating mixtures were procured, and the chemistry of these minerals was obtained using the x-ray fluorescence (XRF) technique. The chemical analysis results are presented in a table (see supplementary Table S1).

To select the composition of different coatings, the composite melting temperature of the coating mixture is the primary requirement. The composite melting temperature of the coating mixture should be less than the melting temperature of the filler wire and base metal. Researchers studied and analyzed the phase diagrams of different systems upon which the coating compositions can be decided. A basic flux system was used with a higher basicity index in this article because basic coatings provide better mechanical properties and low hydrogen diffusion in the welds. Two ternary phase diagrams of CaO-CaF_2-SiO_2 and CaO-SiO_2-Al_2O_3 systems as shown in Fig. 1a and b were used to formulate the 21 sets of flux mixtures. To design an electrode coating composition, the area in the ternary phase diagram was encircled to obtain a lower composite melting temperature (1100–1350°C).[7–11] Using these diagrams the higher and lower ranges of all the coating constituents, CaO, CaF_2, SiO_2 and Al_2O_3, were estimated.
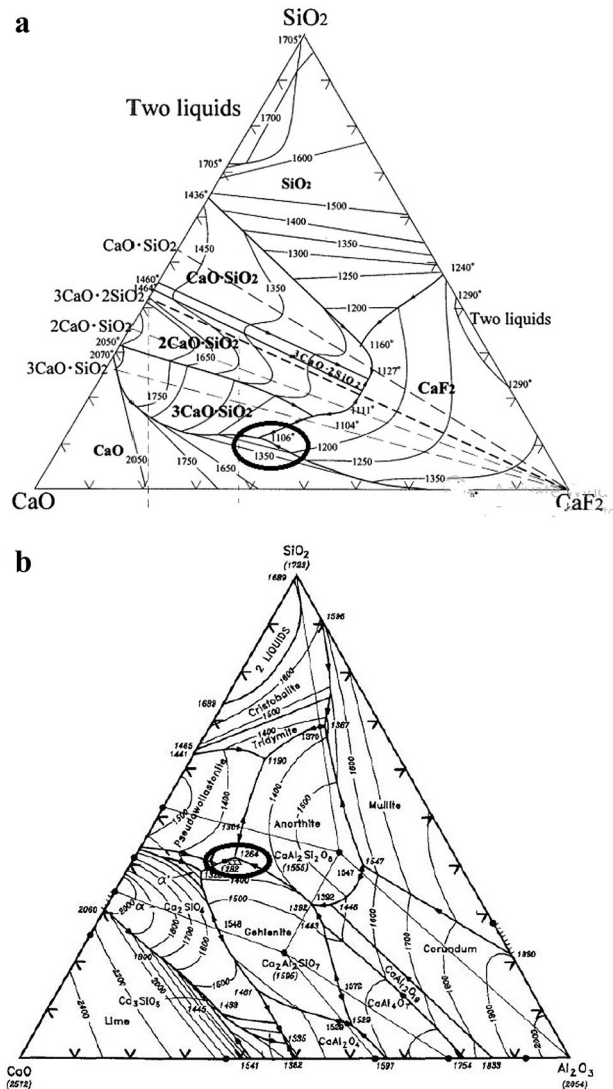

Fig. 1. Ternary phase diagram (experimental): (a) CaO-CaF$_2$-SiO$_2$; (b) CaO-SiO$_2$-Al$_2$O$_3$ system. [Adapted from the figure in Gunner et al. (1993)].[18]

DESIGN OF THE EXPERIMENT AND PREPARATION OF COATINGS

McLean and Anderson[6] suggested an extreme vertices design approach to mixture design. The method suggests that a constrained mixture design for a mixture of n components having lower and upper limits on some or all of the components may be represented mathematically as:

$$0 \le \alpha i \le yi \le \beta \le 100 \tag{1}$$

and

$$\sum_{i=1}^{k} yi = 100 \tag{2}$$

where i = 1, 2, 3,..., n, and α_i and β_i are the lower and upper limits of constants on the y_i, which is the

percentage composition of the ith constituent in the mixture. The upper and lower limits of flux ingredients were determined using ternary phase diagrams and considering the composite melting temperature. Other essential ingredients are important and have to be incorporated so that 25% by weight was reserved. The higher and lower weight limits were scaled down to a total of 75%. The composite coating melting temperature should be less than the melting temperature of the filler wire so a considerable amount of CaF$_2$ was added to decrease the composite melting temperature. Equations 3 and 4 represent the higher and lower percentages of ingredients added to formulate the 21 different electrode coating mixtures, and the total weight of the composition was selected as 75% of the total weight of the electrode coating composition.

$$20 \leq CaF_2 \leq 25$$
$$35 \leq CaF_2 \leq 40$$
$$5 \leq SiO_2 \leq 10 \tag{3}$$
$$1 \leq Al_2O_2 \leq 5$$

$$\sum_{i=1}^{4} xi = 75 \tag{4}$$

By adding the variable proportions of four coating ingredients using the extreme vertices mixture design technique, 21 sets of electrode coating mixtures were obtained. The mixture design space consists of 1 overall body centroid, 12 vertices and

8 centroid as shown in supplementary Fig. S1. The design matrix of 21 sets of electrode composition is shown in Table I.

After obtaining the 21 coating compositions, the minerals available such as calcite, fluorspar, silica and calcinated bauxite were weighed and mixed in the dry mixture. After the proper dry mixing, the potassium silicate was added to the dry mixture of minerals, which will act as a binder and make the mixture wet. This wet mixture was then extruded to the welding filler wires to produce electrodes. Dry coating from the electrodes was collected and crushed and mixed with the help of Muller to perform further experimentation. Twenty-one electrode coatings were developed and characterized using an x-ray diffraction spectrometer (XRD) and Fourier transformed infrared spectrometer (FTIR) to analyze its structural behavior and the different phases present. The density of all the coatings was observed. Thermal gravimetric analysis (TGA) was performed from room temperature to 890°C at a heating rate of 20°C/min to observe the change in enthalpy (ΔH) and weight loss. Thermal properties such as thermal diffusivity, thermal conductivity and specific heat were measured using hot disk apparatus (3.415-mm-size Kapton sensor) for 21 coating compositions.

RESULTS

Density was measured using the bulk density method (mass/volume). For density measurement, the 10-ml cylindrical flask was taken and filled

Table I. Electrode coating composition design matrix (based On CaO-CaF$_2$-SiO$_2$-Al$_2$O$_3$)

Expt. no.	Nature of mixture design point	Ingredients of electrode coatings				Basicity index
		CaO	CaF$_2$	SiO$_2$	Al$_2$O$_3$	
C1	Vertex	25.0	39.5	9.5	1.0	3.36
C2	Vertex	22.5	37.5	10.0	5.0	2.74
C3	Vertex	25.0	38.5	8.5	3.0	3.27
C4	Vertex	24.0	39.0	9.0	3.0	3.23
C5	Vertex	25.0	40.0	7.0	3.0	3.59
C6	Vertex	25.0	40.0	5.0	5.0	3.75
C7	Center of edges	20.0	40.0	10.0	5.0	2.72
C8	Center of edges	24.6	39.6	9.6	1.0	3.3
C9	Center of edges	24.5	40.0	9.5	1.0	3.34
C10	Center of edges	24.5	39.5	10.0	1.0	3.23
C11	Center of edges	24.0	40.0	10.0	1.0	3.23
C12	Center of edges	23.3	38.3	8.3	5.0	3.02
C13	Center of edges	25.0	39.0	10.0	1.0	3.24
C14	Center of edges	25.0	40.0	9.0	1.0	3.45
C15	Center of edges	22.5	40.0	7.5	5.0	3.18
C16	Plane center	22.0	40.0	10.0	3.0	2.96
C17	Plane center	25.0	37.0	10.0	3.0	2.98
C18	Plane center	25.0	35.0	10.0	5.0	2.75
C19	Plane center	23.5	38.5	10.0	3.0	2.97
C20	Plane centre	25.0	37.5	7.5	5.0	3
C21	Overall centroid	23.5	40.0	8.5	3.0	3.44

completely with the coating composition, which represents the volume of the coating composition mixture. The weight of the coating composition mixture contained in the cylindrical flask was measured using an electronic weighing balance. This procedure was repeated three times, and the average values were taken. Table III represents the density values measured for 21 coatings. The minimum density of 1.463 g/cm^3 was obtained for coating composition C18 while the maximum density of 1.585 g/cm^3 was obtained in flux C6. Results obtained for different properties are presented in Tables II–V. Supplementary Figure S2 represents the temperature versus weight plots for electrode coatings C1, C5, C10 and C20, and supplementary Figure S3 represents the plots of heat flow versus temperature.

DEVELOPMENT OF REGRESSION MODELS

Using the design expert tool, regression equations were obtained to consider the individual flux constituents and their interaction mixtures by using the observed properties results, shown in Eqs. 5–10. The ANOVA technique has been utilized to analyze the different regression equations developed (see supplementary Table S2). Table S2 shows that the

Table II. Density of 21 electrode coatings

Coating number	ρ (g/cm^3)
C1	1.55
C2	1.522
C3	1.531
C4	1.52
C5	1.541
C6	1.585
C7	1.556
C8	1.513
C9	1.53
C10	1.555
C11	1.52
C12	1.557
C13	1.579
C14	1.568
C15	1.576
C16	1.521
C17	1.506
C18	1.463
C19	1.558
C20	1.531
C21	1.578

R^2 values are $> 65\%$, which indicates the values are closest to the actual values of the various observed properties shown in supplementary Figure S4.

$$
\begin{aligned}
\text{Density} = {}& -0.75228\,\text{CaO} - 0.20478\,\text{CaF}_2 \\
& - 0.27465\,\text{SiO}_2 - 14.19958\,\text{Al}_2\text{O}_3 \\
& + 0.024391\,\text{CaO}\cdot\text{CaF}_2 \\
& + 0.027773\,\text{CaO}\cdot\text{SiO}_2 \\
& + 0.51868\,\text{CaO}\cdot\text{Al}_2\text{O}_3 \\
& + 0.24531\,\text{CaF}_2\cdot\text{Al}_2\text{O}_3 \\
& + 0.26024\,\text{SiO}_2\cdot\text{Al}_2\text{O}_3 \\
& - 7.08816\text{E}-003\,\text{CaO}\cdot\text{CaF}_2\cdot\text{Al}_2\text{O}_3 \\
& - 8.00216\text{E}-003\,\text{CaO}\cdot\text{SiO}_2\cdot\text{Al}_2\text{O}_3 \\
& - 2.74587\text{E}-003\,\text{CaO}\cdot\text{Al}_2\text{O}_3 \\
& \cdot(\text{CaO}-\text{Al}_2\text{O}_3)\,(\text{reduced cubic model})
\end{aligned}
$$
(5)

$$
\begin{aligned}
\text{Weight loss} = {}& 8.08536\,\text{CaO} + 0.10556\,\text{CaF}_2 \\
& + 2.0011\,\text{SiO}_2 + 4.68607\,\text{Al}_2\text{O}_3 \\
& - 0.16902\,\text{CaO}\cdot\text{CaF}_2 \\
& - 0.33827\,\text{CaO}\cdot\text{SiO}_2 \\
& - 0.25206\,\text{CaO}\cdot\text{Al}_2\text{O}_3 \\
& + 0.10645\,\text{CaF}_2\cdot\text{SiO}_2 \\
& - 8.10068\text{E}-003\,\text{CaF}_2\cdot\text{Al}_2\text{O}_3 \\
& - 0.11205\,\text{SiO}_2\cdot\text{Al}_2\text{O}_3 \\
& (\text{quadratic model})
\end{aligned}
$$
(6)

$$
\begin{aligned}
\text{Change in enthalpy} = {}& 1.09802\text{E}+005\,\text{CaO} \\
& + 38099.18954\,\text{CaF}_2 \\
& + 1.10278\text{E}+005\,\text{SiO}_2 \\
& + 2.95007\text{E}+006\,\text{Al}_2\text{O}_3 \\
& - 3579.75045\,\text{CaO}\cdot\text{CaF}_2 \\
& - 3149.04576\,\text{CaO}\cdot\text{SiO}_2 \\
& - 65699.28707\,\text{CaO}\cdot\text{Al}_2\text{O}_3 \\
& - 2486.30403\,\text{CaF}_2\cdot\text{SiO}_2 \\
& - 73691.08948\,\text{CaF}_2\cdot\text{Al}_2\text{O}_3 \\
& - 60659.6385\,\text{SiO}_2\cdot\text{Al}_2\text{O}_3 \\
& + 1136.42459\,\text{CaO}\cdot\text{CaF}_2\cdot\text{Al}_2\text{O}_3 \\
& + 591.83581\,\text{CaO}\cdot\text{SiO}_2\cdot\text{Al}_2\text{O}_3 \\
& + 805.35673\,\text{CaF}_2\cdot\text{SiO}_2\cdot\text{Al}_2\text{O}_3 \\
& + 360.35492\,\text{CaF}_2\cdot\text{Al}_2\text{O}_3\cdot \\
& (\text{CaF}_2-\text{Al}_2\text{O}_3)(\text{reduced cubic model})
\end{aligned}
$$
(7)

$$\text{Thermal conductivity} = -0.64012\ CaO - 0.36581\ CaF_2$$
$$- 4.51231\ SiO_2$$
$$- 3.17872\ Al_2O_3$$
$$+ 0.024529\ CaO \cdot CaF_2$$
$$+ 0.14208\ CaO \cdot SiO_2$$
$$+ 0.029265\ CaO \cdot Al_2O_3$$
$$+ 0.11074\ CaF_2 \cdot SiO_2$$
$$+ 0.059467\ CaF_2 \cdot Al_2O_3$$
$$+ 0.48011\ SiO_2 \cdot Al_2O_3$$
$$- 2.81985E$$
$$- 003\ CaO \cdot CaF_2.SiO_2$$
$$+ 7.43127E$$
$$- 004\ CaO \cdot CaF_2 \cdot Al_2O_3$$
$$- 6.13732E$$
$$- 003\ CaO \cdot SiO_2.Al_2O_3$$
$$- 8.29734E$$
$$- 003\ CaF2 \cdot SiO_2 \cdot Al_2O_3$$
$$\text{(special cubic model)} \tag{8}$$

$$\text{Thermal diffusivity} = 0.28867\ CaO - 0.2452\ CaF_2$$
$$- 1.91019\ SiO_2 - 4.11901\ Al_2O_3$$
$$+ 0.055093\ CaF_2 \cdot SiO_2$$
$$+ 0.11058\ CaF_2 \cdot Al_2O_3$$
$$+ 0.45079\ SiO_2 \cdot Al_2O_3$$
$$- 0.01132\ CaF_2 \cdot SiO_2 \cdot Al_2O_3$$
$$\text{(reduced special cubic model)} \tag{9}$$

$$\text{Specific heat} = 8.86733\ CaO + 6.08905\ CaF_2$$
$$+ 43.79249\ SiO_2 + 7.02726\ Al_2O_3$$
$$- 0.40077\ CaO \cdot CaF_2$$
$$- 1.60641\ CaO \cdot SiO_2$$
$$+ 0.29181\ CaO \cdot Al_2O_3$$
$$- 1.30345\ CaF_2 \cdot SiO_2$$
$$- 0.42648\ CaF_2 \cdot Al_2O_3$$
$$- 1.69409\ SiO_2 \cdot Al_2O_3$$
$$+ 0.042173\ CaO \cdot CaF_2 \cdot SiO_2$$
$$- 3.55789E - 003\ CaO \cdot CaF_2 \cdot Al_2O_3$$
$$- 0.015796\ CaO \cdot SiO_2 \cdot Al_2O_3$$
$$+ 0.051986\ CaF_2 \cdot SiO_2 \cdot Al_2O_3$$
$$\text{(special cubic model)} \tag{10}$$

DISCUSSION

Effect of Coating Ingredients on Density

Supplementary Table S3 shows that every individual coating ingredient has a significant effect on the density. The SiO$_2$·Al$_2$O$_3$ binary mixture was the only effective constituent having a significant effect on density, while the other binary mixtures have an anti-synergistic effect. Ternary mixtures do not show any effect on the density of this coating formulation. The coefficient of variance has the lower value (CV = 1.38) and represents the good reliability and precise conduct of the experimentation. The model was checked with the special cubic approach and was not significant indicating the ($p > F = 1.143$), which means the F value is large and has an 11.43% chance. By using the backward analysis, the model design was modified. Slag-metal reactions take place during the welding process with coated electrodes. SiO$_2$ and Al$_2$O$_3$ oxides are known as a network former, which has an increasing effect on the density of the molten slag. During the welding process, if oxide inclusions in the weld increase it can decrease the fluidity and increase the density because of its capability to form networks. CaO, Al$_2$O$_3$ and SiO$_2$ present in the coating react during the welding and form SiO^{4+} complex ions, which help to reduce the oxide inclusion in the weld and control the fluidity of the weld pool (Eqs. 11 and 12).[19] Also, when the Al reacts with the SiO$_2$ present in the slag, Al$_2$O$_3$ (slag) forms, which improves the slag detachability and reduces the diffusible hydrogen content, and this improves the welding quality by improving the physicochemical properties (Eq. 13).[19]

$$CaO = Ca^{2+} + O^2 \tag{11}$$

$$SiO_2 + 2O^{2-} = SiO_4^{4-} \tag{12}$$

$$2Al + 1.5\ SiO_2(slag) = 3Si + Al_2O_3(slag) \tag{13}$$
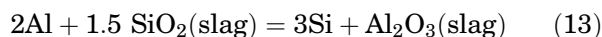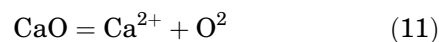
Effect of Coating Mixture Ingredients on Weight Loss

The thermal stability of the electrode coating constituents is a very important aspect in the flux-coated electrode welding. Welding performance and weld quality may be affected because of the thermal instability of the flux constituents.[4] Adverse affects are seen on the slag performance because of the hygroscopic nature (H$_2$O chemically bonded) of the electrode coatings. SiO$_2$ and Al$_2$O$_3$ are the oxides that have a melting temperature $> 1710°C$ and $2072°C$, respectively, which are thermally stable. Table III shows that coating mixture 2 and coating

Table III. Weight loss observation obtained for 21 electrode coating compositions

Exp. no.	Coating	W1 (mg)	W2 (mg)	ΔW = (W1 − W2) (mg)	ΔW (%)
1	C1	11.101	9.436	1.665	14.99
2	C2	11.107	9.678	1.429	12.86
3	C3	9.137	7.728	1.409	15.42
4	C4	12.7	10.911	1.789	14.08
5	C5	8.037	6.816	1.221	15.19
6	C6	11.238	9.66	1.578	14.04
7	C7	7.223	6.263	0.96	13.29
8	C8	9.193	7.795	1.398	15.2
9	C9	12.64	10.913	1.727	13.66
10	C10	8.53	7.261	1.274	14.92
11	C11	11.785	10.211	1.574	13.35
12	C12	10.738	9.176	1.562	14.54
13	C13	7.066	5.876	1.19	16.84
14	C14	8.831	7.516	1.315	14.89
15	C15	7.001	5.86	1.141	16.29
16	C16	8.356	7.204	1.152	13.78
17	C17	10.507	8.984	1.523	14.49
18	C18	9.875	8.31	1.565	15.84
19	C19	12.217	10.523	1.694	13.86
20	C20	11.05	9.39	1.66	15.02
21	C21	12.469	10.73	1.739	13.94

Table IV. Results of ΔH (change in enthalpy) for different electrode coatings

Exp. no.	Coating	Heating rate (°C/min)	Change in enthalpy (ΔH) (J/g)
1	C1	20	− 11,514.7
2	C2	20	− 16,165.2
3	C3	20	− 12,923.8
4	C4	20	− 11,131.7
5	C5	20	− 16,524.2
6	C6	20	− 12,731.5
7	C7	20	− 14,565.2
8	C8	20	− 15,154.8
9	C9	20	− 12,658.2
10	C10	20	− 13,913.3
11	C11	20	− 11,004.1
12	C12	20	− 12,660.2
13	C13	20	− 18,965.8
14	C14	20	− 14,447.8
15	C15	20	− 12,823.1
16	C16	20	− 13,423.1
17	C17	20	− 13,468.5
18	C18	20	− 13,423.1
19	C19	20	− 10,364.2
20	C20	20	− 11,626.9
21	C21	20	− 11,320.9

mixture 7 have lower weight loss compared with the other composition, which contains higher silica and alumina, having higher thermal stability at a higher temperature. Using the DOE approach, it was found that from supplementary Table S3 that individual constituents significantly affect the weight loss of the different coating mixtures, while $CaO \cdot SiO_2$ has a synergistic effect on the weight loss. Other binary mixtures have an anti-synergetic effect on the weight loss of different mixtures. The coefficient of variance is (CV = 6.19%), which indicates a lower value shows the improved precision and reliability. See supplementary Table S2. R^2 (0.77) indicates the changes adjusted for this model are 77% and adjusted R^2 (0.59). The $CaCO_3$ mineral was added to prepare the coating mixture, which is hygroscopic in nature and has a synergetic or increasing effect on the weight loss due to its

Design and Development of Shielded Metal Arc Welding (SMAW) Electrode Coatings Using a
CaO-CaF$_2$-SiO$_2$ and CaO-SiO$_2$-Al$_2$O$_3$ Flux System

2441

Table V. Results of thermal behavior data for 21 electrode coating compositions

Exp. no.	Coating	Thermal conductivity (W/mK)	Thermal diffusivity (mm^2/s)	Specific heat (MJ/m^{3}K)
1	C1	0.3784	0.3691	1.025
2	C2	0.3816	0.3151	1.211
3	C3	0.3888	0.4118	0.9441
4	C4	0.3775	0.4291	0.8799
5	C5	0.3601	0.3523	1.022
6	C6	0.3812	0.3434	1.110
7	C7	0.3893	0.3308	1.177
8	C8	0.3733	0.3081	1.212
9	C9	0.3788	0.3233	1.172
10	C10	0.3874	0.3690	1.050
11	C11	0.3688	0.3684	1.001
12	C12	0.3899	0.3824	1.020
13	C13	0.3653	0.2840	1.286
14	C14	0.3516	0.3088	1.139
15	C15	0.3768	0.3252	1.159
16	C16	0.3848	0.3296	1.167
17	C17	0.3429	0.3058	1.1485
18	C18	0.3756	0.2998	1.208
19	C19	0.3589	0.2942	1.220
20	C20	0.3699	0.3059	1.209
21	C21	0.3921	0.3357	1.168

hygroscopic nature, which leads to a reduction in the viscosity of the slag and increases the chances of contamination with air or moisture. Moisture has a noticeable effect on coating mixtures containing chlorides and fluorides. CaF$_2$ reduces the hygroscopic nature of CaO as previously reported.[28]

Effect of Coating Mixture Ingredients on ΔH (Change in Enthalpy)

Table IV represents the change in enthalpy values of different coating mixtures, which are in negative values; this shows that the nature of the reactions taking place is exothermic, i.e., the coating mixture releases heat. Coating mixture ingredients do not have a significant synergetic effect on enthalpy. CaO·CaF$_2$, SiO$_2$·CaO and Al$_2$O$_3$·SiO$_2$ binary mixtures have an increasing effect and are most effective on the change in enthalpy, while other binary mixtures have synergetic effects. Ternary mixtures CaF$_2$·SiO$_2$ and CaF2·Al$_2$O$_3$(-CaF$_2$-Al$_2$O$_3$) have a synergetic effect on the ΔH, while other ternary constituents have a decreasing effect. Using a mixture design approach, a mathematical model was developed, and it was not significant and revealed only 0.1349% chances for this model to be significant. The backward analysis was used to modify this model; 76.9% of the total variations were adjusted because the R^2 value is (0.769) and the adjusted R^2 (0.668) (see the supplementary Table S2) value is constant and accommodated for this model. The coefficient of variance is (CV = 12.83%). This indicated a lower value depicts the improved precision and better reliability. Table V shows that coating composition 11 has the

minimum value of the change in enthalpy, and coating composition 13 has the maximum value.

Effect of Coating Mixture Ingredients on Thermal Properties

The presence of network-forming chains has a significant effect on the thermal behavior of the fluxes. As the SiO$_2$ content in the welding flux increases, it also increases the thermal conductivity of the fluxes because of the presence of Si^{4+} covalently bonded ions in the network chains.[29,30] The nature of the cations present in the mixture significantly affect the thermal conductivity of the welding fluxes. As suggested by some of the authors, physical and thermal properties were influenced by the non-bridging oxygen available in the system. A significant role of alkaline ions was observed in controlling the thermophysical properties (density, thermal conductivity, thermal expansion and thermal diffusivity) of alumina-silicate-based glasses.[30–33] Regression analysis was performed, and supplementary Table S3 shows linear mixtures have anti-synergetic effects on the thermal conductivity, while the coating composition that contains SiO$_2$ or Al$_2$O$_3$ generally has an effect on the thermal conductivity. Thermal conductivity will be higher if the mixture contains Si4+ ions, which have greater polarization. Coating 2 and coating 7 have a more silica and alumina, and from the experimental analysis, their thermal conductivities are higher compared with other coatings. After developing the mathematical model, it was observed that the thermal conductivity was anti-synergistic and there were only 9.51% chances for this model to be

significant. Backward regression analysis was performed with R^2 (0.75) and adjusted R^2 (0.66). A 2.87% coefficient of variance was observed for this
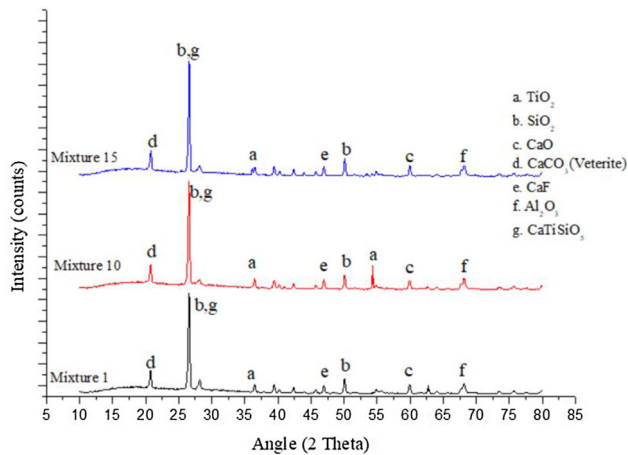
model, which is lower than other properties, describing the good precision and reliability in conducting experiments.

From the regression analysis (supplementary Table S3), it can be concluded that no individual constituent has a significant effect on the thermal diffusivity. $CaO \cdot Al_2O_3$, $CaF_2 \cdot SiO_2$ and $SiO_2 \cdot Al_2O_3$ were found to be the most effective binary mixtures having a significant effect on the thermal diffusivity. $CaO \cdot Al_2O_3 \cdot SiO_2$ is the only mixture (ternary) that significantly increases the thermal diffusivity of the coating mixtures. The model F value (0.197) was observed initially, which showed there were 19.7% chances that the model was significant, and by using backward elimination, the model was modified to reduce noises and the total changes were adjusted with the new R^2 (0.75) (see the supplementary Table S2). The adjusted R^2 was (0.58), which is constant and accommodates the size of the model. A 7.72% coefficient of variance was observed for this model, which is lower than other properties, describing the good precision and reliability in conducting experiments.
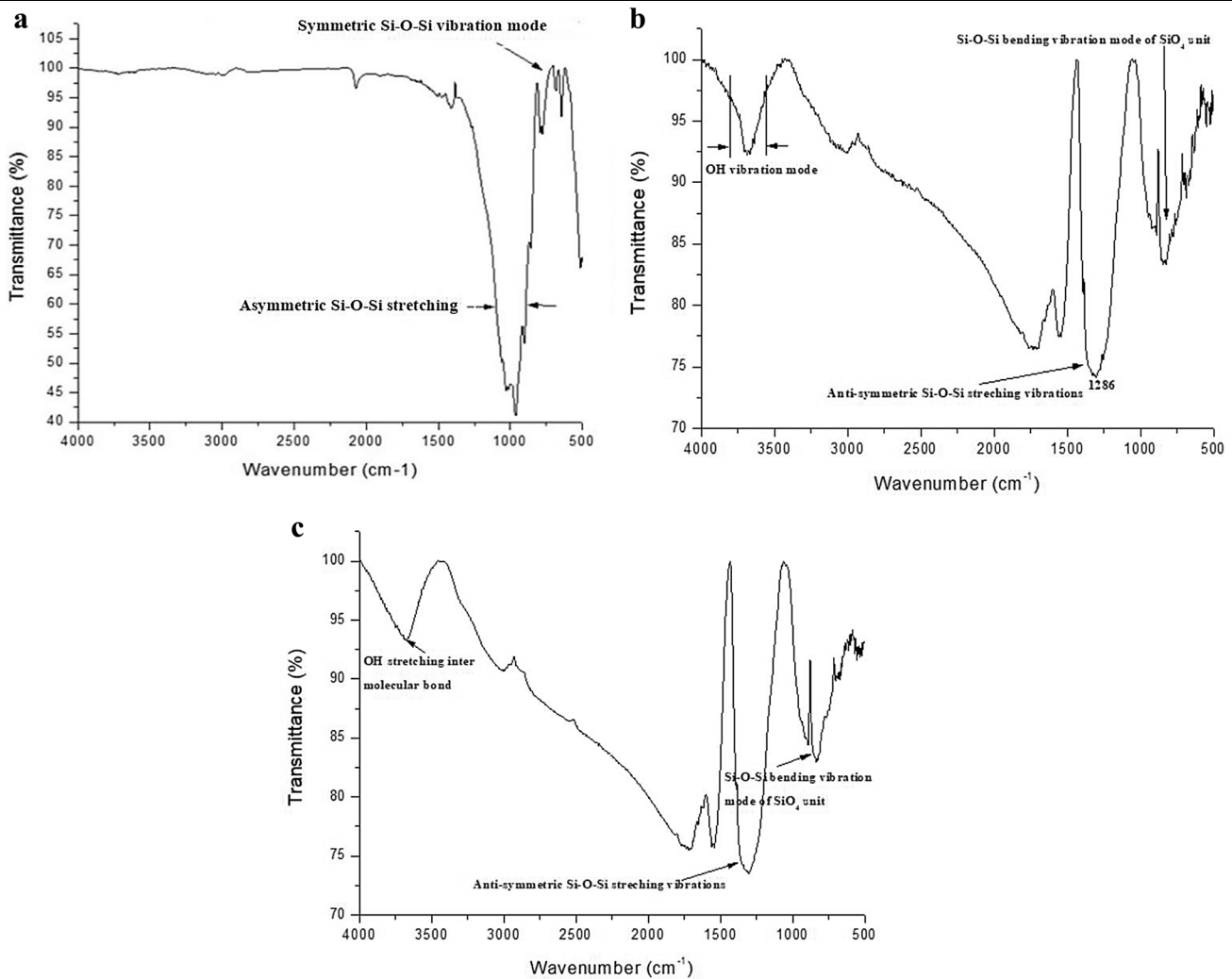

Fig. 2. XRD patterns for coating mixtures C1, C10 and C15.

Fig. 3. FTIR spectra for different coating compositions: (a) C1; (b) C10; (c) C15.

Design and Development of Shielded Metal Arc Welding (SMAW) Electrode Coatings Using a
CaO-CaF$_2$-SiO$_2$ and CaO-SiO$_2$-Al$_2$O$_3$ Flux System

2443

Supplementary Table S3 shows that SiO$_2$·Al$_2$O$_3$ is the most effective (higher F value than the others) binary coating mixture having a synergetic effect on the SH (specific heat). CaO·SiO$_2$ and CaO·Al$_2$O$_3$ also have a significant effect, while only the CaO·CaF$_2$-SiO$_2$ ternary mixture has an increasing effect. From the mathematical model of specific heat, the regression model was revised using backward elimination with the R^2 (0.69) showing that 69% of the total variants are adjusted by this model. The adjusted R^2 (0.52) was also close to the predicted R^2 value. An 8.83% coefficient of variance was observed for this model, which is lower than the other properties, describing the good precision and reliability in the conducting experiments.

XRD and FTIR Analysis of Different Coating Mixtures

A D8 Advance Powder x-ray diffractometer in conjunction with parallel beam geometry is used to carry out the structural analysis of the different coating mixtures developed. XRD plots and phases identified in some of the mixtures are shown in Fig. 2. CaO, CaCO$_3$, CaF$_2$, SiO$_2$ and Al$_2$O$_3$ are the major phases that were present in the coating mixtures. From the XRD analysis, these phases were identified at a different 2θ angles as shown in Fig. 2.

FTIR analysis was performed in the 400–4000 cm^{-1} wave number range at a resolution of $\pm$ 2 cm^{-1} for 33 scans. Information regarding the presence of various bonds among the elements was extracted from the FTIR analysis. FTIR patterns for some of the mixtures are shown in Fig. 3. Due to the presence of the same mixture constituents, the pattern observed in FTIR analysis for different coating compositions is approximately similar with only variations in the peak intensity.

There was a sharp transmission band at $\sim$ 500–700 cm^{-1}, $\sim$ 1250–1400 cm^{-1} and $\sim$ 3500–3750 cm^{-1} for all the coating mixtures. The Al-O bond vibration can be seen at transmission band 586 cm^{-1}. Al$_2$O$_3$ acts as a structural modifier. NBO (non-bridging) oxygen increases with the increase in network former elements and affects the stabilization of the network structure. Silicate anions (SiO$_4^{-4}$) bind together with the network modifier (K$^+$, Li^{2+} and Al^{3+}) by the electrostatic force of attraction and develop an ionic bridge between two non-bridging oxygens. The electrostatic forces between the two types of non-bridging oxygen decrease with the addition of CaO, K$_2$O and BaO network breaker elements, which decreases the thermophysical properties.[31-33]

Contour Surface Plots and Multi-Objective Optimization for Different Properties

Predicted Vs actual values plots indicating the predicted values of thermophysical properties are shown in supplementary Fig. S4. Variations in different properties were observed in different regions of plots, so a constant value of thermal properties was given by every contour curve marked on the surface, and each dotted point on the plot indicates 1 of the 21 mixture design points. Supplementary Fig. S5 shows contour plots for different properties for different proportions of the ingredients CaO, CaF$_2$, SiO$_2$ and Al$_2$O$_3$.

Optimization was performed to minimize the density, thermal diffusivity and weight loss and maximize the thermal conductivity and specific heat, keeping the change in enthalpy (ΔH) in a range. The optimization problem is developed as a nonlinear, multivariable and multiobjective problem. The complex desirability optimization method proposed by Derringer and Suich[32] was used to optimize these properties. In multiobjective optimization, weights are applied to fix the effect of feedback.[4,7-11] In this study, the problem was to improve the physicochemical properties to get the best optimum values of properties. Optimized solutions were found (see the supplementary Table S4) at various levels of desirability with an equal weight-age for weight loss, density, thermal conductivity, specific heat, thermal diffusivity and ΔH (change in enthalpy).

Four-electrode coating compositions were randomly selected, and the developed regression models of different properties were validated. See supplementary Table S5 and Table S6, which represent the observation data, and the error percentages of all the properties studied are < 5%, which are under the acceptance range.

CONCLUSION

Electrode coatings were designed using extreme vertices design methods by adding different constituents (CaO, CaF$_2$, SiO$_2$ and Al$_2$O$_3$) in different proportions. Regression models for different properties were developed. Conclusions drawn from this article are:

- The individual coating mixture constituents do not affect the thermal properties but have an effect on density and weight loss.
- Density is affected by the individual mixture constituents. CaO·Al$_2$O$_3$ is the most effective mixture, which has a synergetic effect on the density, while other binary constituents have a decreasing effect.
- The weight loss of electrode-coating compositions was affected by the individual as well as binary components. The CaO·SiO$_2$ binary mixture constituent has the most pronounced effect on weight loss, while CaO·CaF$_2$ and CaF$_2$·Al$_2$O$_3$ have a decreasing effect. Weight loss is also due to the presence of moisture in the coating mixtures. CaO is one of the important mixture ingredients, which reduces the moisture content in the weld pool by providing a gaseous shield and helps to reduce the defects in the welds.
- No individual coating constituent had any significant effect, but binary and ternary compo-

nents affect the change in enthalpy. $CaO \cdot CaF_2$, $CaO \cdot SiO_2$ and $SiO_2 \cdot Al_2O_3$ are the binary mixtures that have increasing effects on the change in enthalpy. $CaO \cdot CaF_2 \cdot Al_2O_3$ is the only ternary component that has a synergetic effect on the change in enthalpy.

- $CaO \cdot SiO_2$, $CaO \cdot Al_2O_3$ and $CaF_2 \cdot SiO_2$ binary mixtures have an increasing effect on thermal conductivity, but the $SiO_2 \cdot Al_2O_3$ binary mixture is most effective and has a significant effect on the thermal conductivity. The ternary mixture $CaF_2 \cdot SiO_2 \cdot Al_2O_3$ has a synergetic effect, while the other ternary components have a decreasing effect.

- $CaF_2 \cdot SiO_2$, $CaF_2 \cdot Al_2O_3$ and $SiO_2 \cdot Al_2O_3$ binary mixtures have a significant effect on the thermal diffusivity. The ternary mixture $CaF_2 \cdot SiO_2 \cdot Al_2O_3$ is the most influencing component, which affects the thermal diffusivity of the mixture and increases the thermal diffusivity.

- $CaO \cdot CaF_2$, $CaO \cdot SiO_2$ and $SiO_2 \cdot Al_2O_3$ binary mixtures have a significant effect, and $SiO_2 \cdot Al_2O_3$ is the most effective binary mixture, which has an increasing effect on the specific heat. The ternary mixture $CaO \cdot CaF_2 \cdot SiO_2$ was the only mixture that had a synergetic effect on the specific heat, while the other ternary components had an anti-synergistic effect on the specific heat.

ELECTRONIC SUPPLEMENTARY MATERIAL

The online version of this article (https://doi.org/10.1007/s11837-019-03494-9) contains supplementary material, which is available to authorized users.

REFERENCES

1. K. Sham and S. Liu, *Weld. J.* 93, 271 (2014).
2. T.H. North, H.B. Bell, and A. Nowicki, *Suppl. Weld. J.* 229, 63s (1978).
3. A. Joseph, K.R. Sanjai, and J.T. Murgann, *Press. Vessels Pip.* 82, 700 (2005).
4. L. Sharma, R. Chhibber, *IMechE Part E J. Process Mech. Eng.* 0(0), 1 (2018).
5. J.H. Palm, *Weld. J.* 51, 358s (1972).
6. R.A. McLean and V.L. Anderson, *Technometrics* 8, 447 (1966).
7. D. Bhandari, R. Chhibber, and N. Arora, *J. Manuf. Process.* 23, 61 (2016).
8. D. Bhandari, R. Chhibber, and N. Arora, *Mater. Sci. Forum* 880, 37 (2017).
9. D. Bhandari, R. Chhibber, N. Arora, *IMechE Part L J. Mater. Des. Appl.* 0(0), 1 (2016).
10. S. Jindal, R. Chhibber, and N.P. Mehta, *IMechE Part B J. Eng. Manuf.* 227, 383 (2013).
11. S. Jindal, R. Chhibber, and N.P. Mehta, *IMechE Part B J. Eng. Manuf.* 228, 1259 (2014).
12. M. Ushio, B. Zaghloul, and W. Metawally, *Transactions of JWRI* 24, 45 (1995).
13. T.W. Eagar, *Weld Res. Suppl.* 22, 76s (1978).
14. C.A. Natalie and D.L. Olson, *Ann. Rev. Mater. Sci.* 16, 389 (1986).
15. R. Qin and G. He, *Metall. Mater. Trans. A* 44A, 1475 (2012).
16. H. Wang, R. Qin, and G. He, *Metall. Mater. Trans. A* 47A, 4530 (2016).
17. R.C. DeVries, R. Roy, and F. Osborn, *J. Am. Ceram. Soc.* 38, 158 (1955).
18. G. Eriksson and A.D. Pelton, *Metall. Mater. Trans. A* 24, 807 (1993).
19. P.A. Burke, J.E. Indacochea, and D.L. Olson, *Weld J.* 69, 115 (1990).
20. C.B. Dallam, S. Liu, and D.L. Olson, *Weld J.* 64, 140 (1985).
21. K. C. Mills, "Estimation of slag properties", Southern African Pyrometallurgy (Short course), March 2011.
22. S. Sridhar, K.C. Mills, O.D.C. Afrange, H.P. Lorz, and R. Carli, *Ironmak. Steelmak.* 27, 238 (2000).
23. K.C. Mills, Y. Su, A.B. Fox, Z. Li, R.P. Thackray, and H.T. Tsai, *ISIJ Int.* 45, 619 (2005).
24. J.H. Kim, R.H. Frost, D.L. Olson, and M. Blander, *Weld. Res. Suppl.* 69, 446s (1990).
25. U. Mitra and T.W. Eagar, *Metall. Mater. Trans. A* 22B, 83 (1991).
26. L. Sharma and R. Chhibber, *Ceram. Int.* 45, 1569 (2019).
27. L. Sharma, R. Chhibber, Silicon, https://doi.org/10.1007/s12633-019-0068-5.
28. P. Kanjilal, T.K. Pal, and S.K. Majumdar, *Weld. J.* 86, 135s (2007).
29. K.C. Mills and S. Seethharaman, *Fundamentals of metallurgy* (Abington: Woodhead Publishing, 2005). ISBN-10: 1-84569-094-X.
30. M. Kerstan, M. Muller, and C. Russel, *Mater. Res. Bull.* 46, 2456 (2011).
31. Y.P. Tarlakov, I.F. Es'kova, A.M. Shevyakov, Issled Strukt Sostyaniya Neorg Veshchestu 1, 7 (1974).
32. G. Kaur, M. Kumar, A. Arora, O.P. Pandey, and K. Singh, *J. Non Cryst Solids* 357, 858 (2011).
33. M. Garai, N. Sasmal, A.R. Molla, and B. Karmakar, *Solid State Sci.* 44, 10 (2015).